

## STUDY OF THICKNESS DEPENDENT CHARACTERISTICS OF $\text{Cu}_2\text{S}$ THIN FILM FOR VARIOUS APPLICATIONS

M. Ramya<sup>1\*</sup>, and S. Ganesan<sup>2</sup>

\* rams\_thangam@yahoo.co.in

Received: December 2010

Accepted: May 2011

<sup>1</sup> Department of Physics, Sri Shakthi Institute of Engg. & Tech., Coimbatore 641 062, Tamil Nadu, India.

<sup>2</sup> Department of Physics, Government College of Technology, Coimbatore 641 013, Tamil Nadu, India.

**Abstract:** Different thickness of  $\text{Cu}_2\text{S}$  thin films were prepared by vacuum evaporation under a pressure of  $10^{-6}$  torr at an evaporation rate of  $3\text{\AA}/\text{sec}$ .  $\text{Cu}_2\text{S}$  has direct band gap energy and indirect band gap energy at  $1.2\text{eV}$  and  $1.8\text{eV}$  respectively. This paper presents the analysis of structural and optical properties of the  $\text{Cu}_2\text{S}$  thin film by X-ray diffractometer (XRD) and UV-Vis-NIR Spectrophotometer. XRD studies showed polycrystallinity of  $\text{Cu}_x\text{S}$  thin films at higher thickness. Optical spectra of  $\text{Cu}_2\text{S}$  film exhibit high transmittance in the visible region and high absorbance in the near infra-red region. Moreover, the optical property of the film confirms that transmission mainly depends on the thickness of the film. Structural and resistivity property reveals that  $\text{Cu}_2\text{S}$  film at higher thicknesses shows slight deviations in stoichiometry. Possible applications of the  $\text{Cu}_2\text{S}$  thin films are also discussed.

**Keywords:** Thin Film - $\text{Cu}_2\text{S}$ - Vacuum Evaporation- Resistivity- Structural property

### 1. INTRODUCTION

Recent investigations have evoked considerable interest in  $\text{Cu}_2\text{S}$  thin film because of its extensive potential applications in solar cells, photo thermal conversions of solar energy as solar absorber coating [1], electro conductive coatings [2], solar control coatings[3], microwave shielding coatings and as sensors[4]. It has also been used in air-glass tabular solar collectors as absorber coating in photodetector and photovoltaic applications [5].  $\text{Cu}_2\text{S}$  thin films are efficiently used in solid junction solar cells that have many applications as it is a direct conversion device.  $\text{Cu}_2\text{S}$  is known to be excellent heterojunction partner with CdS. Much attention has been focused on thin film CdS/ $\text{Cu}_2\text{S}$  heterojunction due to their great promise as a low cost solar power converter owing to their high efficiency with improved stability.

Copper Sulphide is known to exist in several crystallographic and stoichiometric forms which comprise chalcocite ( $\text{Cu}_2\text{S}$ , orthorhombic), djurlite ( $\text{Cu}_{1.96}\text{S}$ , orthorhombic), digenite ( $\text{Cu}_{1.8}\text{S}$ , orthorhombic), anilite ( $\text{Cu}_{1.75}\text{S}$ , orthorhombic) and co-vellite ( $\text{CuS}$ , hexagonal) [5].  $\text{Cu}_2\text{S}$  thin film has been prepared by several deposition techniques such as chemiplating [6], Solid State Reaction [7], Sputtering [8], Spray Pyrolysis [9,10], Flash Evaporation, photochemical method

[11,12] and Vacuum evaporation method[13]. Copper Sulphide has been investigated both in bulk and thin film form with regards to its structural, resistivity, optical and electronic properties. These properties are largely governed by the composition of  $\text{Cu}_x\text{S}$  which in turn is governed by the method of preparation and the deposition conditions prevailing during growth. The purpose of this research is therefore to report the characteristics of  $\text{Cu}_2\text{S}$  thin films as a function of film thickness prepared by vacuum evaporation. Vacuum evaporation is the technique used to deposit variety of materials by heating a source material under vacuum until it evaporates. The compounds evaporate congruently and dissociate completely on evaporation. It is the low energy process, with high purity and simplicity.

### 2. EXPERIMENTAL

$\text{Cu}_2\text{S}$  of different thicknesses were deposited on properly cleaned flat glass substrates under the pressure of  $10^{-6}$  torr. Constant rate of evaporation  $3\text{\AA}/\text{sec}$  was maintained throughout the sample preparation. Rotary drive is employed to maintain uniformity in film thickness. The substrate to source distance was optimized to be at 18.1 cm inside the vacuum chamber. The thicknesses of the film were measured by quartz

crystal monitor. High purity (99.99%) copper sulphide powder was utilized for evaporation.

Structural analyses of copper sulphide film were carried out using X-ray diffractometer (Shimadzu XRD-6000). Samples mounted on the specimen holder using silica gel were scanned at a rate of 0.50/min with  $\text{CuK}\alpha$  radiation. The radiation was filtered using a 10 divergence slit, a  $1^\circ$  slatter slit and a 0.15 mm receiving slit. All the films were analyzed in the  $20\text{-}80^\circ$  ( $2\theta$ ) scale angle range. The interplanar spacing  $d_{hkl}$  can be calculated using the Bragg's relation

$$d_{hkl} = \frac{n\lambda}{2\sin\theta} \quad (1)$$

where 'n' is the order of reflection, ' $\theta$ ' is the angle of incidence relative to the planes and 'd' is the distance between the atomic planes parallel to the axis of the incident beam. The grain size (D) was evaluated from full width at half maximum ( $\beta$ ) of dominant diffraction peak for selected samples. This was done by using scherrer's formula

$$D = \frac{k\lambda}{\beta \cos\theta} \quad (2)$$

Where 'k' is the correction factor with value 0.9, ' $\lambda$ ' is the x-ray wavelength (1.5406 for  $\text{CuK}\alpha$ ) and ' $\theta$ ' is the bragg angle. The influence of thickness on the strain ( $\varepsilon$ ) of the deposited film were also determined using the following expression

$$\varepsilon = \frac{\beta \cos\theta}{4} \quad (3)$$

The dislocation density ( $\delta$ ) can be related with grain size as follows

$$\delta = \frac{1}{D^2} \quad (4)$$

where 'D' is the grain size of the film.

The resistivity of  $\text{Cu}_2\text{S}$  thin films were analyzed using four point probe method. The arrangement consists of PID controlled oven (model-PID-200 scientific equipment and services, Roorkee, India) in combination with low current source (model-LCS-01) and digital micro voltmeter. Resistivity of the films were

calculated using the formula

$$\rho = \rho_0 \exp(E_g/KT) \quad (5)$$

Where ' $\rho$ ' is resistivity, ' $\rho_0$ ' is constant, 'K' is the Boltzmann constant, 'T' is the absolute temperature and ' $E_g$ ' is the activation energy.

UV-Vis-NIR Spectrophotometer is used for optical measurements. The spectrophotometer has wavelength in the range 190 nm to 2500 nm with an accuracy of 0.3 nm. This spectrophotometer is interfaced with the computer and the recorded spectrum is obtained from the computer. The measured absorbance (A) of the film is related to transmittance (T) by  $A = \log(1/T) = (I_0/I)$ , where 'I' is the transmitted light and ' $I_0$ ' is the incident light. The absorption coefficient ( $\alpha$ ) is related to band gap ( $E_g$ ) by

$$\alpha h\nu = (h\nu - E_g)^{1/2} \text{ for direct transition and } \quad (6-1)$$

$$\alpha h\nu = (h\nu - E_g)^2 \text{ for indirect transition } \quad (6-2)$$

where ' $\nu$ ' is the frequency of the incident light and 'h' is the Planck's constant. Extrapolating the straight line portion of the plot of  $(\alpha h\nu)^2$ ,  $(\alpha h\nu)^{1/2}$  against  $h\nu$  to the energy axis for zero absorption co-efficient the optical band gap of the material can be determined. The refractive index 'n' of the film can be expressed by the classical relation

$$n = \frac{1}{2t(\frac{1}{\lambda})} \quad (7)$$

where ' $\lambda$ ' is the wavelength of the incident radiation and 't' is the thickness of the film.

### 3. RESULTS AND DISCUSSION

#### 3.1. Structural Analyses

Figure 1 and 2 shows the XRD pattern of  $\text{Cu}_2\text{S}$  thin film of 1000  $\text{\AA}$  and 7000  $\text{\AA}$  thickness respectively. XRD pattern of Figure1 reveals the mixed state of amorphous and polycrystalline nature of the film at 1000  $\text{\AA}$  thickness. The presence of prominent peaks at  $2\theta = 46.3, 27.7$  in Figure 2 clearly indicates the polycrystalline nature of the film at higher thickness. Thus it is

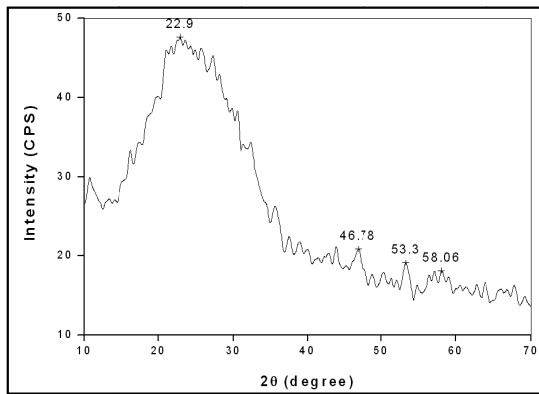


Fig. 1. XRD pattern of Cu<sub>2</sub>S thin films of 1000 Å thickness

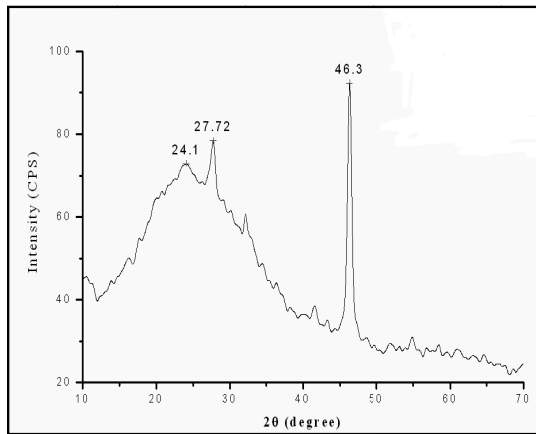


Fig. 2. XRD pattern of Cu<sub>2</sub>S thin films of 7000 Å thickness

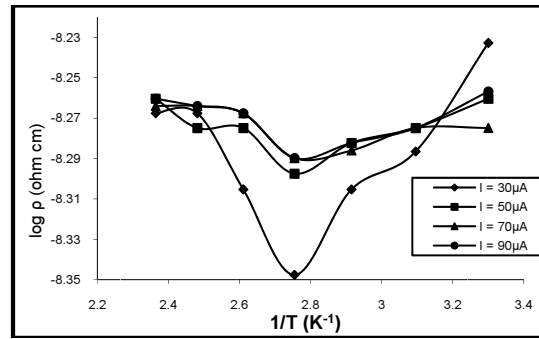


Fig. 3. Variation of resistivity with Inverse of temperature for Cu<sub>2</sub>S film of 1000 Å thickness

observed that at higher thickness, the Cu<sub>2</sub>S thin film shows slight deviations from stoichiometry.

The ‘d’ spacing values are calculated and the peak positions observed for the Cu<sub>2</sub>S thin films are in good agreement with standard JCPDS (ICSD 200986) value of hexagonal Cu<sub>2</sub>S. The structural parameters such as grain size (D), strain (ε) and dislocation density (δ) are calculated using (2,3,4) respectively and the values are reported in Table1 along with ‘d’ spacing values.

The interplanar distance is found to be a=5.94 Å, c= 9.64 Å which shows a slight difference with the values (a=3.95 Å, c=6.78Å) reported for Cu<sub>2</sub>S films. This difference in values is due to the lattice mismatch. The calculated value of grain size shows that with a systematic increase in film thickness, Cu<sub>2</sub>S thin film shows decreases in the value of grain size. This smaller

Table 1. Structural parameter of Cu<sub>2</sub>S films for different thicknesses.

| Thickness (Å) | Lattice d- spacing (Å) |              | hkl planes | Crystalline size (D) (nm) | Strain (ε)10 <sup>-4</sup> lines <sup>-2</sup> m <sup>-4</sup> | Dislocation density (δ) 10 <sup>14</sup> lines/m <sup>2</sup> |
|---------------|------------------------|--------------|------------|---------------------------|--|---|
|               | Standard               | Experimental |            |                           |  |   |
| 1000          | 1.9870                 | 1.9701       | 110        | 207.59                    | 1.7439   | 23.2  |
| 3500          | 1.9870                 | 1.9750       | 110        | 138.40                    | 2.615  | 52.2  |
| 5000          | 1.9790                 | 1.9808       | 110        | 19.773                    | 18.309   | 0.255   |
| 7000          | 1.9790                 | 1.9803       | 110        | 103.79                    | 3.4879   | 92.8  |

grain size is due to the formation of new grains over older ones [14,15]. However the particles grew bigger when the films were synthesized at higher thickness.

### 3. 2. Resistivity Analyses

The variation of resistivity versus inverse of absolute temperature with various currents (30-90 $\mu$ A) for samples of lower thickness is shown in Figure 3. The critical temperature called as transition temperature is estimated within (383K-403K) by using the relation (5).The film showed semi conductive behavior at lower temperature and metallic above critical temperature and agrees with the earlier reports on Cu<sub>2</sub>S thin films [16,17].

Figure 4 depicts the change in resistivity with temperature for Cu<sub>2</sub>S thin films of different thicknesses. Resistivity tends to increase as the film thickness increases from 1000  $\text{\AA}$  to 5600 $\text{\AA}$ ,

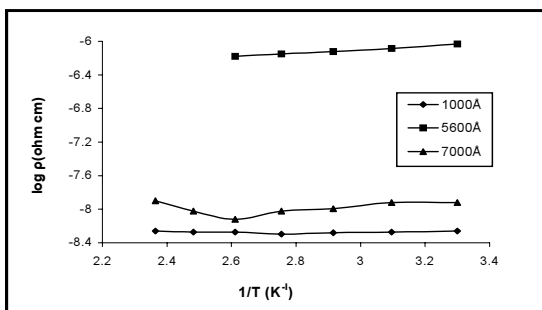


Fig. 4. Variation of resistivity with inverse of temperature for Cu<sub>2</sub>S films of different thicknesses measured at constant current

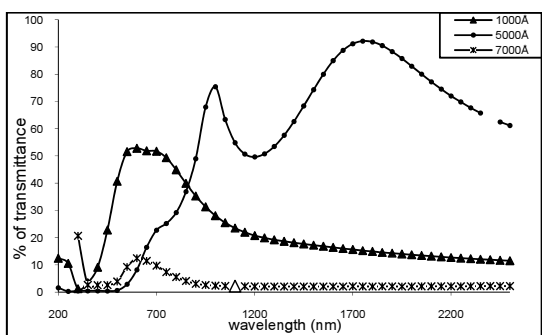


Fig. 5. Variation of transmittance spectra with wavelength for Cu<sub>2</sub>S films of different thicknesses

and further resistivity decreases at higher thickness. This observation is attributed to the non- stoichiometric composition of the films at higher thickness [13,18] which is similar to the earlier results reported in this paper. The decrease in resistivity of the film at higher thickness reveals that the film has high conductivity at higher thickness that could be suitable for solar cell applications.

### 3. 3. Optical Analyses

The optical transmittance spectra of Cu<sub>2</sub>S thin films of different thicknesses measured as a function of wavelength of incident photons is shown in Figure 5. The transmission curve shows two regions, the shorter wavelength region, and the longer wavelength region [19]. In the shorter wavelength region the transmission increases with wavelength, while in the near infrared

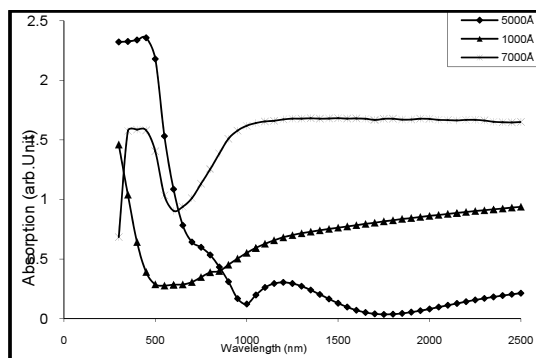


Fig. 6. Variation of absorbance spectra with wavelength for Cu<sub>2</sub>S films of different thicknesses

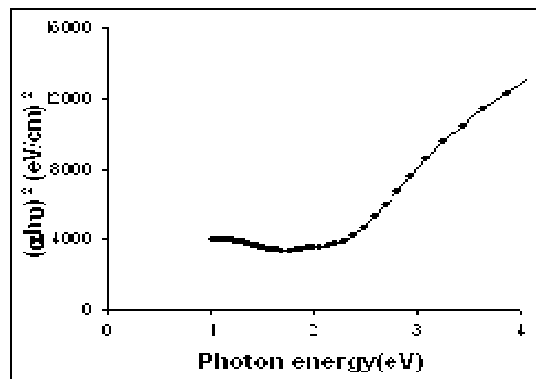


Fig. 7. Plot of  $(\alpha h \nu)^2$  versus  $h \nu$  for Cu<sub>2</sub>S thin film of 1000 $\text{\AA}$  thickness showing direct edge at 1.8 eV.

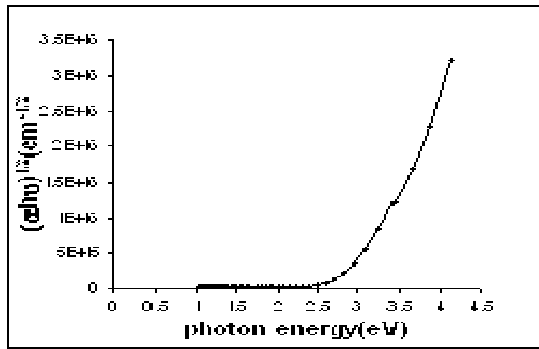


Fig. 8. Plot of  $(\alpha h \nu)^2$  versus  $h \nu$  for  $\text{Cu}_2\text{S}$  thin film of 1000Å thickness showing indirect edge at 2.9 eV.

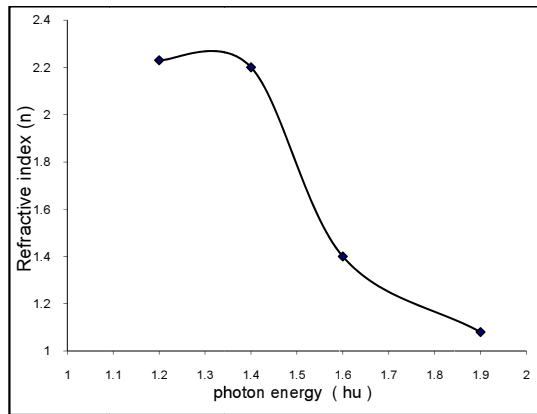


Fig. 9. Refractive index variation with photon energy for  $\text{Cu}_2\text{S}$  films

region transmission decreases with wavelength [13]. The transmission in the shorter wavelength region is due to interband transitions from valence band towards the conduction band, whereas in the higher wavelength region the transmission is due to free carriers. This  $\text{Cu}_2\text{S}$  film in the visible region matches the phototropic vision of human eye ( $\sim 5500\text{\AA}$ ) which makes them suitable for solar control coatings on architectural windows and automobiles in the regions with warm climates [3]. Transmission is more remarkable at lower thicknesses, while at the same time, a substantial decrease of transmission is found in higher thickness. Lower thickness  $\text{Cu}_2\text{S}$  films with high transmittance are suitable for solar thermal devices and eyeglass coatings to reduce solar reflectance and increases transmittance of glass. Low

transmittance  $\text{Cu}_2\text{S}$  films could be used for anti dazzling coatings for car windscreens and driving mirrors to reduce the dazzling effects of light at night [20]. From Figure 6 it is clear that  $\text{Cu}_2\text{S}$  film has high absorbance at higher thickness [21] and the films synthesized with high absorbance, relatively low transmittance could be useful for the construction of poultry houses.

The Figure 7, 8 shows the  $(\alpha h \nu)^2$ ,  $(\alpha h \nu)^{1/2}$  against ' $h \nu$ ' curve for direct and indirect transitions of  $\text{Cu}_2\text{S}$  thin film of lower thickness respectively. All films exhibit two distinct absorption regions: a high energy threshold and low energy threshold region, possibly corresponding to two absorption mechanisms [22]. A sharp decrease in the range (3 to 4 eV) indicates the first threshold and a gradual decrease in the range (1.5 to 2.5 eV) shows second threshold region. The optical band gap of the film estimated from the graph is reported in Table 2. From Table2 it is inferred that both direct and indirect transition showed thickness dependence characteristics of  $\text{Cu}_2\text{S}$  thin film. In general thickness dependence of band gap can arise due to the following causes (i) large density of dislocations (ii) height of the crystalline films. The refractive index ' $n$ ' as a function of photon energy for  $\text{Cu}_2\text{S}$  thin film is shown in Figure 9. The film shows a refractive index variation from 2.4 to 2 in the lower photon energy range and from 1.4 to 1 in the higher photon energy range. Moreover using (7) the refractive index for different film thickness has been calculated and are reported in Table 3. From Table 3 it is observed that refractive index is proportional to film thickness. It is also concluded that  $\text{Cu}_2\text{S}$  thin film of lower thickness has very low refractive

Table 2. Variation of band gap with film thickness

| Thickness (Å) | Optical band gap (eV) |                        |
|---------------|-----------------------|------------------------|
|               | $(\alpha h \nu)^2$    | $(\alpha h \nu)^{1/2}$ |
| 1000          | 1.8                   | 2.9                    |
| 5000          | 1.4                   | 2.1                    |
| 7000          | 1.2                   | 1.8                    |

**Table 3.** Variation of Refractive index with film thickness

| Thickness<br>(Å) | Refractive index<br>(n) |
|------------------|-------------------------|
| 1000             | 1.08                    |
| 3500             | 1.4                     |
| 5000             | 2.2                     |

index value and the film with such low refractive index value could find applications in antireflection coatings.

#### 4. CONCLUSION

XRD studies were used to obtain structural characterizations of  $\text{Cu}_2\text{S}$  thin film. Resistivity studies revealed that the film showed a semi-conducting nature up to 403 K, above which they showed a metallic behavior.  $\text{Cu}_2\text{S}$  films coated at lower thickness has high transmittance with low resistance, whereas films at higher thickness has low transmittance. Increase in thickness of copper sulphide thin film leads to decrease in the value of 'x' in  $\text{Cu}_x\text{S}$  film. Low thickness copper sulphide film could be useful in solar thermal devices and eyeglass coatings, those with higher thickness could be useful in anti dazzling coatings.

#### ACKNOWLEDGEMENT

The author is grateful to Dr.R.Sathyamoorthy, Kongunadu Arts and Science College, Coimbatore, for his suggestions and support to carry out this work.

#### REFERENCES

- Nair, P. K., and Nair, M. T. S., "Chemically Deposited SnS- $\text{Cu}_x\text{S}$  Thin Films With High Solar Absorptance: New Approach to All-Glass Tubular Solar Collectors", J. PHY., D, Appl. Phy. 1991,24, 83-88.
- Yamamoto, T., Kubota, E., Taniguchi, A., Dev,

- S., Tanaka, K., and Osakada, K., "Electrically Conductive Metal Sulfide-Polymer Composites Prepared by Using Organosols of Metal Sulfides", Chem.Mater. 1992, 4, 570-576
- Nair, M. T. S, and Nair, P. K., "Chemical Bath Deposition of  $\text{Cu}_x\text{S}$  Thin Films and Their Prospective Large Area Applications", Semicond.Sci.Technol., 1989,4,191-199.
- Sagade, A. A., and Sharma, R., "Copper Sulphide ( $\text{Cu}_x\text{S}$ ) as an Ammonia Gas Working at Room Temperature", Sensors and Actuators B: Chemical ,2008 ,133, 135-143.
- Pathan, H. M., Desai, J. D., and Lokhande, C. D., "Modified Chemical Deposition and Physio-Chemical Properties of Copper Sulphide( $\text{Cu}_2\text{S}$ ) Thin Films", Appl. Surf. Sci., 2002,202, 47-56.
- Vedel, J., Cowache, P., and Soubeyran, M., "Electroplating of  $\text{Cu}_x\text{S}$  on Cds", Solar Energy Materials ,1984,10,25-34.
- Burgelman ,M. and Vos, A., De,"Evaporation of CuCl and  $\text{CuCl}_2$  for the Fabrication of  $\text{Cu}_x\text{S}$  /CdS Thin Film Solar Cells",Thin Solid Films ,1983,102,367-374
- He, Y. B., Polity, A., Österreicher, I., Pfisterer, D., Gregor, R., Meyer, B. K., and Hardt, M., "Hall Effect and Surface Characterization of  $\text{Cu}_2\text{S}$  and CuS Films Deposited by RF Sputtering", Physica B: Condensed Matter,2001, 308-310,1069-1073.
- Wang, S. Y., Wand, W. and Lu, Z. H., "Asynchronous – Pulse Ultrasonic Spray Pyrolysis Deposition of  $\text{Cu}_x\text{S}$ (X=1,2) Thin Films",Mater.Sci.Eng.,B ,2003,103, 184-188.
- Isac, L., Duta, A., Kriza, A., Manolache, S., and Nanu, M., "Copper Sulfides Obtained by Spray Pyrolysis — Possible Absorbers in Solid-State Solar Cells", Thin Solid Films , 2007,515, 5755–5758.
- Santheep K., Mathew, Rajesh, N. P., Masaya Ichimura and Udayalakshmi, "Preparation and Characterization of Copper Sulphide Particles by Photochemical Method", Materials Letters , 2008, 62, 591-593.
- Ichimura, M., Takeuchi, K., Nakamura, A. and Arai, E., "Photochemical Deposition of Se and CdSe Films From Aqueous Solutions",Thin Solid Films , 2001,384,157-159.
- Couve, S. , Gousskov, L., Szepessy, L., Vedel, J.,

- and Castel, E., "Resistivity and Optical Transmission of  $\text{Cu}_x\text{S}$  Layers as a Function of Composition", *Thin Solid Films*, 1973, 15, 223-231.
14. Lalitha, S., Sathyamoorthy, R., Senthilarasu, S., Subbarayan, A. and Natarajan, K., "Characterization of CdTe Thin film-Dependence of Structural and Optical Properties on Temperature and Thickness", *Solar Energy Materials and Solar Cells*, 2004, 82, 187-199.
  15. Loptez Otero, A., "The Dependence of Grain Size of Continuous Epitaxial Films on the Growth Conditions", *Journal of Crystal Growth*, 1977, 42, 157-159.
  16. Ramya, M. and Ganesan, S., "Annealing Effects on Resistivity Properties of Vacuum Evaporated  $\text{Cu}_2\text{S}$  Thin Films", *International Journal of Pure and Applied Physics*, 2010, 6, 243-249.
  17. Lokhande, C. D., Pathan, H. M., Giersig, M. and Tributsch, H., "Preparation of  $\text{ZnX}(\text{O},\text{S})_y$  Thin Films Using Modified Chemical Bath Deposition Method", *Appl. Surf. Sci.*, 2002, 187, 101-107.
  18. Duchemin, S., Youm, I., Bougnot, J. and Cadene, M., "Fabrication and Characterization of Sprayed  $\text{Cd}_{1-y}\text{Zn}_y\text{S}-\text{Cu}_2\text{S}$  (dry process) Solar Cell", *Solar Energy Materials*, 1987, 15, 337-350.
  19. Vanhoecke, E. and Burgelman, M., "Reactive Sputtering of Thin  $\text{Cu}_2\text{S}$  Films for Application in Solar Cells", *Thin Solid Films*, 1984, 112, 97-106.
  20. Ilenikhena, P. A., "Comparative Studies of Improved Chemical Bath Deposited Copper Sulphide ( $\text{CuS}$ ) and Zinc Sulphide ( $\text{ZnS}$ ) Thin Films at 320K and Possible Applications", *African Physical Review*, 2008, 2:0007, 59-67.
  21. Engelken, R. D. and Mc Cloud, H. E., "Electrodeposition and Material Characterization of  $\text{Cu}_x\text{S}$  Films", *J. Electrochem. Soc.*, 1985, 132, 567-573.
  22. Rastogi, A. C. and Salkalachen, S., "Optical Absorption Behavior of Evaporated  $\text{Cu}_2\text{S}$  Thin Films", *Thin Solid Films*, 1982, 97, 191-199.